ChemComm

COMMUNICATION

View Article Online
View Journal | View Issue



Cite this: *Chem. Commun.*, 2022, **58**, 3174

Received 21st January 2022,
Accepted 7th February 2022

DOI: 10.1039/d2cc00414c

rsc.li/chemcomm



# Anhydrous calcium phosphate crystals stabilize DNA for dry storage†

Philipp L. Antkowiak, [a] Julian Koch,[a] Przemyslaw Rzepka, [ab] Bichlien H. Nguyen,[c] Karin Strauss,[c] Wendelin J. Stark [a] and Robert N. Grass *[a]

**The resilience of ancient DNA (aDNA) in bone gives rise to the preservation of synthetic DNA with bioinorganic materials such as calcium phosphate (CaP). Accelerated aging experiments at elevated temperature and humidity displayed a positive effect of co-precipitated, crystalline dicalcium phosphate on the stability of synthetic DNA in contrast to amorphous CaP. Quantitative PXRD in combination with SEM and EDX measurements revealed distinct CaP phase transformations of calcium phosphate dihydrate (brushite) to anhydrous dicalcium phosphate (monetite) influencing DNA stability.**

The degradation of DNA is important for various areas of science and technology, including molecular biology,[1] medicine,[2] archeology[3,4] and more recently, digital data storage.[5,6] First investigations of the chemical decay of genetic material started soon after the revelation of the structure of DNA in the 1950s, paving the way for today's diverse interest in DNA.[7–9] Since decay conditions are manifold and highly dependent on environmental factors, there is no unanimous model on decay kinetics. However, dominant pathways include oxidation, hydrolysis and methylation.[2] In archeology, progress in DNA purification and extraction technologies as well as new sampling sites have very recently pushed the record for the oldest sequenced genome to 1.65 million years,[4] consistent with experimental calculations.[3,10] Such aDNA extracted from bone and tooth fossils still holding information after long periods, shows the ability of bioinorganic materials to massively increase the durability of DNA. Several technical solutions to enhance the stability of DNA molecules have been reported, ranging from simple drying procedures on Whatman filter paper,[11] various sugar matrices,[12–14] inorganic salts,[15] carrier DNA or RNA[16,17] to more elaborate nanoparticle encapsulates,[5,18,19] anoxic environments,[20] as well as co-storage with drying agents such as phosphorus pentoxide.[12,13]

One specific application of DNA, for which long-term stability is required, is its possible use as a storage medium for the world's ever-increasing amount of data. The molecule has proven to be an excellent data carrier due to its density and universal format.[21–23] Expected data densities surpass several exabyte per gram,[21,24] which is orders of magnitude higher than current non-volatile storage media. For automatized, long-term storage of DNA-encoded data[25,26] extensive cooling and liquid handling steps are not practical due to high energy and infrastructure cost. A simple solution, without the use of elaborate multi-step preparations to enhance DNA stability, has not yet been found. The efficient preservation of aDNA in bone supports the idea of using bioinorganic materials such as CaP, although the effect of the material on the stability of DNA is only poorly understood. Few studies provide quantitative data on the interaction between bone and DNA.[27] Most work assumes that the adsorption of DNA onto hard, connective tissue is the reason for the stability of DNA in archaeological samples.[28] Also, in biotechnology CaP is widely used to co-precipitate DNA for an efficient transfection process due to an increased *in vitro* DNA stability,[29–31] increased melting temperatures,[32] and further engineered CaP nanoparticles show a better transfection performance.[33,34] Building on these observations, we here investigate the structure and durability of DNA co-precipitated with CaP for dry storage. We show enhanced stability of DNA in crystalline CaP using powder X-ray diffraction (PXRD) including Rietveld refinement to identify phase compositions, scanning electron microscopy (SEM) and infrared spectroscopy (DRIFTS).

The synthesis of encapsulated model DNA with CaP was performed by co-precipitating an equimolar mixture of $KH_2PO_4/K_2HPO_4$ and $CaCl_2$ in the presence of DNA at pH 6, to yield $Ca[PO_3(OH)]\cdot 2H_2O$ (brushite) and KCl (sylvite), exhibiting a Ca/P ratio of 1. We chose this system because it provides favorable synthesis conditions in conjunction with DNA at a high weight loading of 18 wt% (see Fig S1, ESI† and previously published data[15]) and allows consistent and controlled production of crystalline calcium phosphate. Other calcium phosphate

[a] *Institute for Chemical and Bioengineering, Department of Chemistry and Applied Biosciences, ETH Zurich, Vladimir-Prelog-Weg 1, 8093 Zürich, Switzerland. E-mail: robert.grass@chem.ethz.ch*
[b] *Laboratory for Catalysis and Sustainable Chemistry, Paul Scherrer Institute, Forschungsstrasse 111, 5232 Villigen, Switzerland*
[c] *Microsoft Research, 1 Microsoft Way, Redmond, WA 98052, USA*

† Electronic supplementary information (ESI) available. See DOI: 10.1039/d2cc00414c

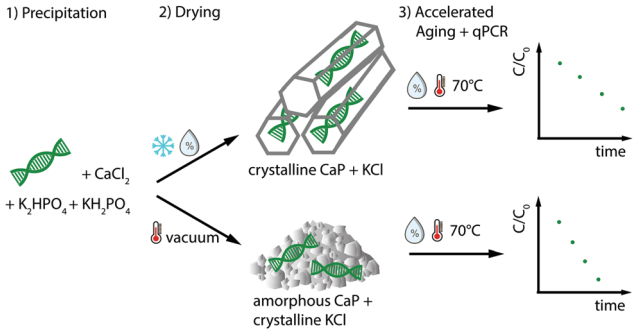


Fig. 1 Scheme summarizing the workflow of stability testing. Synthetic DNA was precipitated in the presence of $CaCl_2$, $K_2HPO_4$ and $KH_2PO_4$. The samples were dried at 4 °C and 65% relative humidity (RH), resulting in crystalline CaP (brushite) and KCl or at 45 °C under vacuum, which gave amorphous CaP and crystalline KCl. The change of DNA concentration in accelerated aging experiments at 70 °C and 50% RH were subsequently measured with qPCR.

compositions were not obtainable at temperature and pH conditions compatible with DNA, and our initial tests showed no increase in DNA stability (see Fig. S2, ESI†) with other precipitation compositions. Fig. 1 shows an overview of the conducted experiments with Ca/P = 1. Since PXRD and DRIFTS require sample amounts in the milligram range, we chose to use genomic salmon testes DNA, which can be obtained in larger amounts than the synthetic DNA (sDNA) usually handled for DNA storage applications. For qPCR experiments, we employed synthetic, double-stranded DNA with a length of 148 bp as this is the format in which data is optimally preserved.[5] In order to have both model DNAs as similar as possible, the genomic DNA was sheared with ultrasonication, which yielded an average length of 100 bp. Thus, the two DNA sources are comparable in length and structure (dsDNA), and only differ in nucleotide sequence. We exposed the CaP/DNA co-precipitates to different drying conditions and recorded PXRD patterns to reveal differences in crystallinity, resp. material composition. Fig. 2a shows the patterns for the same precipitation reaction, dried in two different ways. Samples dried for 30 min at 45 °C under vacuum (<20 mbar, referred to as "quickly dried") mainly feature reflections belonging to sylvite (KCl), which forms as a byproduct from mixing calcium chloride and the potassium hydrogen phosphates. As indicated in Fig. 2a, Rietveld refinements show two small and broad peaks around 33°$\theta$ assigned to monetite. We therefore assume that major parts of calcium phosphate in this sample are in a disordered (amorphous) state. This is supported by the electron micrographs displaying the absence of identifiable crystals, independent of the used DNA source (gDNA and sDNA). Slowing down the crystallization process by increasing humidity to 65% and lowering the temperature to 4 °C for 5 days (referred to as "slowly dried") increased the amount of ordered phase of the material, showing the formation of brushite. This trend is also observable in samples precipitated in the absence of DNA (Fig. S8, ESI†). Also, in contrast to the quickly dried samples, characteristic needle like structures are visible in the electron micrographs, independent of the DNA source utilized. Additional images are shown in the ESI.† The formation of brushite

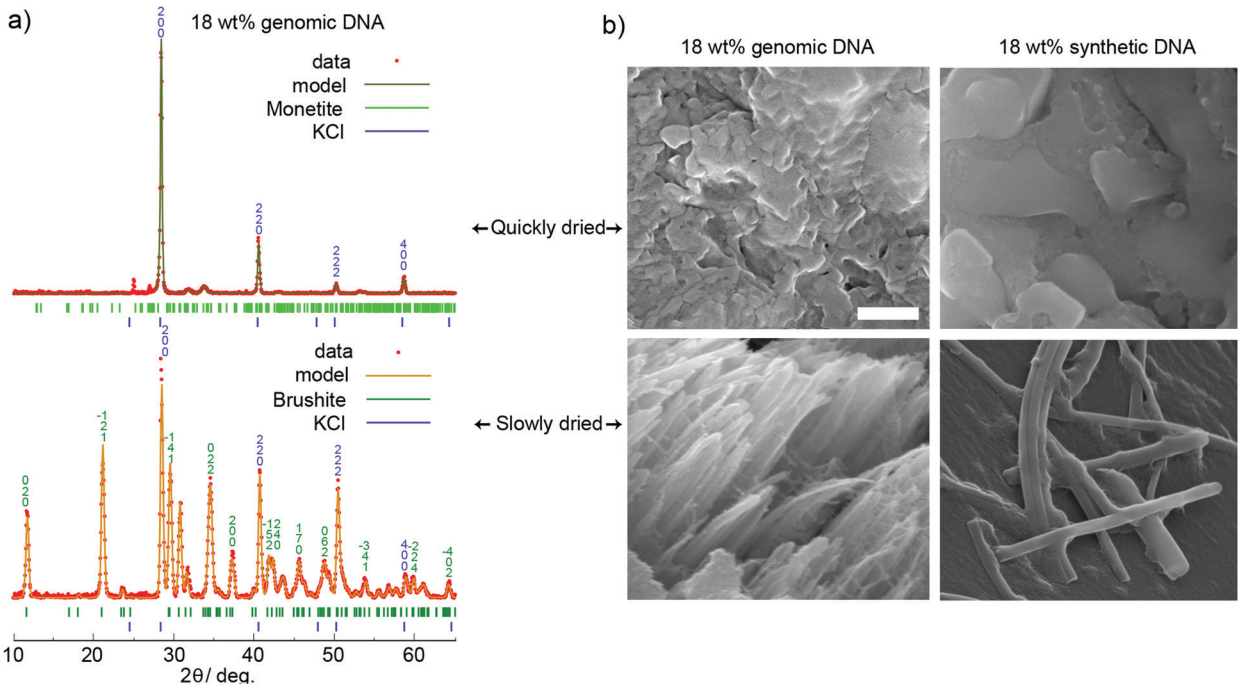


Fig. 2 (a) PXRD patterns and fitted models of salmon testes DNA in CaP with precipitates quickly dried (upper diffractogram) and slowly dried (lower diffractogram). Miller indices are indicated at the corresponding reflection. (b) SEM micrographs of genomic and synthetic DNA in CaP dried both ways. For slowly dried samples, characteristic needle-shaped brushite crystals are visible which do not occur in quickly dried samples. The scale bar denotes a length of 500 nm.

over monetite can be explained by the sufficient amount of water present during the drying process. The fitted data did not reveal any other major calcium phosphate or amorphous phases. The intensities for single reflections in the PXRD of KCl and brushite varied due to preferred orientation of the measured crystal powders according to March-Dollase.[35]

To investigate the stability of the co-precipitated synthetic DNA in CaP, we performed rapid aging experiments.[5] For this, dried co-precipitates of synthetic DNA in CaP with 18 wt% DNA were exposed to 70 °C and 50% RH for up to 6 days and DNA decay was measured by qPCR (Fig. 3). During the first day, all samples show a similar degree of degradation. Subsequently, DNA in crystalline CaP (orange squares) exhibited an increased stability compared to DNA in rapidly dried CaP (brown dots). The latter moreover degraded with about the same rate as DNA in the absence of CaP. Notably, after 5 days, the concentration of DNA protected in crystalline CaP was close to three orders of magnitude higher. To better understand the influence of CaP crystal structure under the measurement conditions, we determined the change in crystal structure after various time intervals at 70 °C and 50% RH, corresponding to the accelerated aging conditions. After 10 hours, essentially all brushite originally in the sample (65.9% brushite, remainder sylvite) was transformed to monetite (see Fig S6–S8 ESI†), which is favored at temperatures above 60 °C.[36] Our data moreover shows that during aging over four days, monetite is also formed in the quickly dried samples, however with less crystallinity (Fig. S8 ESI†).

Considering the observed decay rates and PXRD data, the stabilizing effect for DNA can be attributed to monetite, which forms more rapidly in the slowly dried samples and presumably prevents hydrolytic damage to dried DNA due to its anhydrous crystal structure. Therefore, the decay rates should be compared after the initial phase transition of brushite to monetite, as indicated in Fig. 3.

To shed more light on the local distribution of genomic DNA in CaP, an electron dispersive X-ray analysis (EDX) was conducted. Fig. 4 shows element maps of a representative spot displaying cubic-shaped sylvite and needle-structured brushite crystals. Intensities of phosphorus and nitrogen are slightly more pronounced in the vicinity of calcium, which shows that DNA can be predominantly found close to CaP. This is in good agreement to studies investigating DNA's affinity to CaP under various conditions[27,37] and depicts the close interaction between the phosphate bearing biopolymer and the calcium phosphate structures. The observations of crystal structure changes during drying and aging are confirmed by DRIFTS measurements of genomic DNA in CaP (Fig. S9, ESI†): For slowly dried DNA in CaP the FTIR spectrum closely resembles the spectra of CaP precipitated in the absence of DNA, with characteristic peaks at 1650, 1215, 1139, 1005, 986 and 874 $cm^{-1}$, all characteristic for brushite.[38] For quickly dried samples, significantly less structure is observable. This shows that upon rapid drying, the organization of calcium phosphate to form homogeneous species is hindered by the presence of the biopolymer. This trend persists with aging of the samples for 4 days at 70 °C (see additional DRIFT spectra in Fig. S10 ESI†).

Above data shows that DNA encapsulated in well-ordered monetite structures is protected from decay. The interaction of the phosphate DNA backbone with the calcium ions of the crystal and the absence of free water from this crystal structure may be of importance to prevent hydrolytic damage. Still, the format investigated here differs from the naturally occurring bone samples comprising ancient DNA, which mainly consist of calcium-deficient hydroxyapatite (HAp, Ca/P ratio 1.67) embedded in a collagen matrix. It would be of great interest

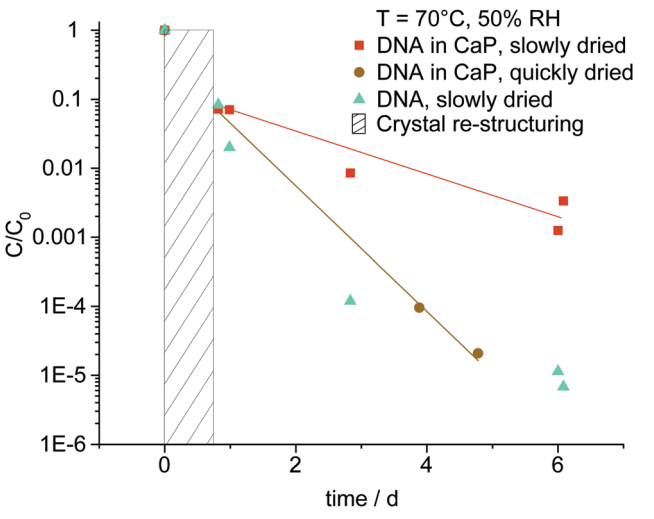


Fig. 3 Relative concentration of 18 wt% DNA in CaP quickly and slowly dried with pure DNA as control samples, measured after a phase of crystal re-structuring (hatched). Accelerated aging conditions comprised 70 °C and 50% RH. The red and brown lines are a guide for the eye. DNA decay in crystalline CaP is slowed down compared to DNA in amorphous CaP.

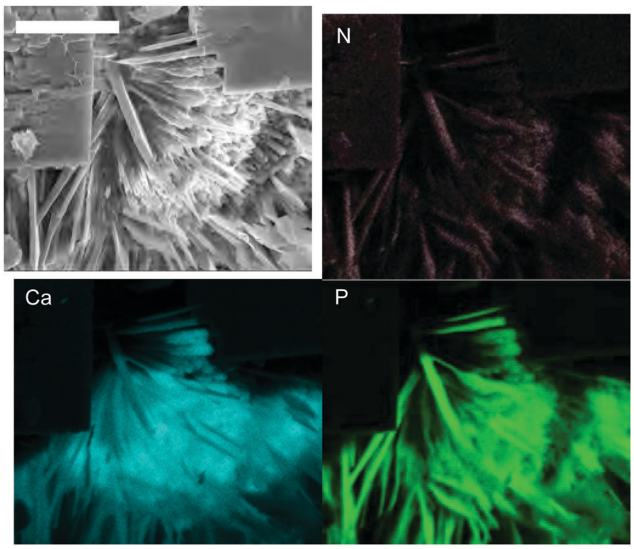


Fig. 4 EDX element maps of calcium (Ca), phosphorus (P) and nitrogen (N) for a representative spot of slowly dried DNA in CaP. The scale bar denotes a length of 50 μm. The contrast in the element maps was increased for clarity.

to investigate and compare the stability of DNA encapsulated in synthetic HAp with monetite. However, due to elevated pH and temperature ranges required to form crystalline HAp[39–43] no synthesis procedure compatible with DNA could be identified, and initial attempts forming non-crystalline CaP with Ca/P = 1.67 did not yield an increased DNA stability (see Fig. S2, ESI†). However, it may be expected that DNA encapsulated in natural HAp crystals similarly profits from the absence of free water in the crystal structure as well as the strong interaction between the phosphate backbone of DNA and the calcium ions of the inorganic crystals.

In search for a simple, solid-state storage format for DNA, we have shown the importance of CaP crystal structure on the thermal stability of DNA. We found a stabilizing effect through calcium phosphate dried at low temperature and high relative humidity (brushite), which undergoes a structural change to monetite at 70 °C. DNA protection with wet salt chemistry features a facile encapsulation and release process compared to more elaborate methods such as silica nanoparticle encapsulates or anoxic capsules. CaP-DNA precipitates are amenable to full automation, which is paramount for scalable DNA data storage applications. While the control of crystal structure has clear advantages in this respect, the long drying time of 5 days, control of humidity and temperature during that time and the presumably rigid peak stability performance around 18 wt% need to be considered for further applications. However, this simple, bottom-up synthesis of DNA salt encapsulates shows the potential of bio-inspired, inorganic materials for solid-state, room-temperature storage of DNA. From our analyses we hypothesize a correlation between the monetite crystal structure and qPCR detectable damage, showing a positive influence on stability for crystalline compared to amorphous CaP. The facile synthesis and drying procedure provide accessible tools for dense and stable room temperature storage of DNA. Our study shows the capability of salt-based storage solutions featuring high-loading, which further drives the technology towards automatized, long-term preservation of digital data stored in DNA.

We would like to thank Michael Wörle for the help with XRD analysis and Microsoft for funding.

## Conflicts of interest

B. H. N. and K. S. are Microsoft employees.

## References

1 J. H. Houtgraaf, J. Versmissen and W. J. van der Giessen, *Cardiovasc. Revasc. Med.*, 2006, **7**, 165–172.
2 T. Lindahl, *Instability and decay of the primary structure of DNA*, 1993.
3 M. E. Allentoft, *et al.*, *Proc. R. Soc. B*, 2012, **279**, 4724–4733.
4 T. van der Valk, *et al.*, *Nature*, 2021, **591**, 265–269.
5 R. N. Grass, R. Heckel, M. Puddu, D. Paunescu and W. J. Stark, *Angew. Chem., Int. Ed.*, 2015, **54**, 2552–2555.
6 L. Organick, *et al.*, *Small Methods*, 2021, **5**, 1–10.
7 W. Ginoza and B. H. Zimm, *Proc. Natl. Acad. Sci. U. S. A.*, 1961, **47**, 639–652.
8 S. Greer and S. Zamenhof, *J. Mol. Biol.*, 1962, **4**, 123–141.
9 T. Lindahl and B. Nyberg, *Biochemistry*, 1972, **11**, 3610–3618.
10 L. Orlando, *et al.*, *Nature*, 2013, **499**, 74–78.
11 R. Guthrie, *JAMA*, 1961, **178**, 863.
12 B. Shirkey, *et al.*, *Nucleic Acids Res.*, 2003, **31**, 2995–3005.
13 J. Bonnet, M. Colotte, D. Coudy, V. Couallier, J. Portier, B. Morin and S. Tuffet, *Nucleic Acids Res.*, 2009, **38**, 1531–1546.
14 S. Smith and P. A. Morin, *Optimal Storage Conditions for Highly Dilute DNA Samples: A Role for Trehalose as a Preserving Agent*, Griffith University Technical Report, 2005, 5.
15 A. X. Kohll, P. L. Antkowiak, W. D. Chen, B. H. Nguyen, W. J. Stark, L. Ceze, K. Strauss and R. N. Grass, *Chem. Commun.*, 2020, **56**, 3613–3616.
16 A. Baoutina, S. Bhat, L. Partis and K. R. Emslie, *Anal. Chem.*, 2019, **91**, 12268–12274.
17 T. Köhler, A. K. Rost and H. Remke, *Biotechniques*, 1997, **23**, 722–726.
18 D. Paunescu, M. Puddu, J. O. Soellner, P. R. Stoessel and R. N. Grass, *Nat. Protoc.*, 2013, **8**, 2440–2448.
19 W. D. Chen, *et al.*, *Adv. Funct. Mater.*, 2019, **29**, 1901672.
20 S. Tuffet and D. G. De Souza, Pat. WO2009115761A2, 2011.
21 G. M. Church, Y. Gao and S. Kosuri, *Science*, 2012, **337**, 1628.
22 N. Goldman, P. Bertone, S. Chen, C. Dessimoz, E. M. Leproust, B. Sipos and E. Birney, *Nature*, 2013, **494**, 77–80.
23 L. Organick, *et al.*, *Nat. Biotechnol.*, 2018, **36**, 242–248.
24 S. M. Tabatabaei Yazdi, Y. Yuan, J. Ma, H. Zhao and O. Milenkovic, *Sci. Rep.*, 2015, **5**, 1–10.
25 C. N. Takahashi, B. H. Nguyen, K. Strauss and L. Ceze, *Sci. Rep.*, 2019, **9**, 1–5.
26 S. Newman, A. P. Stephenson, M. Willsey, B. H. Nguyen, C. N. Takahashi, K. Strauss and L. Ceze, *Nat. Commun.*, 2019, **10**, 1–6.
27 A. Grunenwald, C. Keyser, A. M. Sautereau, E. Crubézy, B. Ludes and C. Drouet, *Appl. Surf. Sci.*, 2014, **292**, 867–875.
28 M. J. Collins, *et al.*, *Archaeometry*, 2002, **44**, 383–394.
29 D. Lou and W. M. Saltzman, *Nat. Biotechnol.*, 2000, **18**, 33–37.
30 M. Urabe, A. Kume, K. Tobita and K. Ozawa, *Anal. Biochem.*, 2000, **278**, 91–92.
31 H. Boulaiz, J. A. Marchal, J. Prados, C. Melguizo and A. Aránega, *Cell. Mol. Biol.*, 2005, **51**, 3–22.
32 M. Banik and T. Basu, *Dalton Trans.*, 2014, **43**, 3244–3259.
33 E. V. Giger, J. Puigmartí-Luis, R. Schlatter, B. Castagner, P. S. Dittrich and J. C. Leroux, *J. Controlled Release*, 2011, **150**, 87–93.
34 F. Ridi, I. Meazzini, B. Castroflorio, M. Bonini, D. Berti and P. Baglioni, *Adv. Colloid Interface Sci.*, 2017, **244**, 281–295.
35 W. A. Dollase, *J. Appl. Crystallogr.*, 1986, **19**, 267–272.
36 Y. Kim, S. Y. Lee, Y. Roh, J. Lee, J. Kim, Y. Lee, J. Bang and Y. J. Lee, *J. Nanosci. Nanotechnol.*, 2015, **15**, 10008–10016.
37 J. J. van den Beucken, X. F. Walboomers, S. C. Leeuwenburgh, M. R. Vos, N. A. Sommerdijk, R. J. Nolte and J. A. Jansen, *Acta Biomater.*, 2007, **3**, 587–596.
38 A. Hirsch, I. Azuri, L. Addadi, S. Weiner, K. Yang, S. Curtarolo and L. Kronik, *Chem. Mater.*, 2014, **26**, 2934–2942.
39 M. Sadat-Shojai, M. T. Khorasani, E. Dinpanah-Khoshdargi and A. Jamshidi, *Acta Biomater.*, 2013, **9**, 7591–7621.
40 S. V. Dorozhkin, *Biomatter*, 2011, **1**, 121–164.
41 K. Ioku, G. Kawachi, S. Sasaki, H. Fujimori and S. Goto, *J. Mater. Sci.*, 2006, **41**, 1341–1344.
42 H. Zhang and B. W. Darvell, *Acta Biomater.*, 2011, **7**, 2960–2968.
43 R. Z. LeGeros and J. P. LeGeros, in *Dense Hydroxyapatite*, World Scientific, 1993, pp. 139–180.